EXTRACTING ROCK INFORMATION BASED ON INTEGRATED CONVOLUTIONAL NEURAL NETWORK AND IMAGE PROCESSING TECHNOLOGY

Jiangying Wang[1], Yun Zhou[2], and Miaofen Huang[3*]

[1]Guangdong Ocean University, No. 1, Haida Road, Mazhang District, Zhanjiang, 524088, China, Email: 1361748619@qq.com

[2]Guangdong Ocean University, No. 1, Haida Road, Mazhang District, Zhanjiang, 524088, China, Email: 1282854954@qq.com

[3]Guangdong Ocean University, No. 1, Haida Road, Mazhang District, Zhanjiang, 524088, China, Corresponding author: hmf808@163.com

KEY WORDS: Lithology identification; Oil content extraction; Convolutional neural network; Model integration; Comprehensive image-processing techniques

ABSTRACT: The lithology identification and the extraction of oil-bearing information on rock surface are the most critical works in exploring minerals, oil and gas resources. An automatic classification method of integrated convolutional neural network was proposed to identify the lithology of rocks. Comprehensive image-processing techniques are used to extract the oil-bearing information on the rock surface. Firstly, five convolutional neural network models, including AlexNet, VGG16, Inception_V3, Xception and ResNet50, were trained with the enhanced rock sample set to obtain five different classification models. An integrated model was further established by using the majority voting method; Secondly, the rock area in the image, which was taken in a dark box illuminated by fluorescent light, was extracted by the comprehensive image-processing techniques, such as linear stretching, Canny edge detection, and image expansion, and verification was made with the area of interest extracted by ENVI; Finally, the ratio of oil-bearing area to the area of the rock was calculated by the image masking and HSV transformation processes. The classification results show that the verification accuracy of a single model (Inception_V3) is 98.87%, while the verification accuracy of the integrated model (Xception, VGG16, Inception_V3) is 99.29%, which is better than single model; In addition, the deviation of the rock profile obtained by the comprehensive image-processing techniques fall within 1% compared with the area of interest drawn by ENVI; The percentage of the pixel number of oil-bearing derived from the results processed by the image mask and HSV transformation processes to the total pixel number of the rock area is 2.85%. Compared with the traditional observation procedure, the workflow used in the paper can save time greatly to extract the oil-bearing information.

1. Introduction

The identification of rock is an essential task in the exploration of oil, gas and mineral resources. Rock lithology includes rock colour, structure, composition, unique minerals, etc. The traditional methods of identifying rock include seismic, gravity and magnetic, logging, remote sensing, electromagnetic, geochemistry, hand specimens and rock thin slice analysis (Zou et al, 2020). Rock slice analysis is the main identification method, but it is limited in accuracy and time cost, as well as human subjective factors (Cheng et al, 2017).

Many scholars of geology have applied machine learning to the identification of rocks. Ren, et al. (2021) used the over 300G rock images to train the residual neural network, constructed a rock identification model and developed an intelligent rock identification tool, which provides convenience for geologists. Bai, et al. (2019) collected 1000 images of each type of rock for 6 common rock types and realized the identification of rock images by constructing the VGG16 model. Zhang, et al. (2018) built a deep learning transfer model based on small sample data and a convolutional neural network, using transfer learning methods. The results showed that the model has good generalization ability. Hu, et al. (2020) took the rock images collected by the network as input, constructed a bilinear convolutional neural network model, and tried to fundamentally improve the identification rate of rock images based on the fine-grained identification of rock images. Cheng, et al. (2018) trained the Deep Belief Network based on the 4800 rock images in the Ordos Oilfield area. The accuracy rate of 1200 test images was 94.75%, indicating that the DBN model is highly effective for fine-grained identification. Polat, et al. (2021) explored the best combination of two models and four optimizers, and experiments show that DenseNet121 uses RMSprop to obtain the highest accuracy when identifying rock images. Feng, et al. (2019) comprehensively considered the global information and local information of the rock image, used the twin convolutional neural network to extract the global feature and local feature of the rock image. In this way, the identification of rock images can be realized. The above research shows that machine learning has a good effect on the classification of rock images, but it is limited to the learning ability of a single model.

Therefore, this paper proposes a rock image identification method based on the convolutional neural network ensemble model. The ensemble model is based on the idea of ensemble learning. Through a particular method (voting method, average method, learning method), the output results of each trained model are synthesized to obtain a better performance multi-fusion model. Li, et al. (2021) integrated models such as gated cycle unit, XGBoost, and random forest to predict the NOx emissions of a power plant, and the mean square error was reduced by 13.350% to 52.186% compared with the single model. Feng, et al. (2019) applied model integration and transfer learning methods to identify tree species images in complex backgrounds, with an accuracy rate of 99.15%. Zhang, et al. (2017) proposed a bad image identification method based on deep model integration and achieved good results in detecting bad information, with an identification accuracy of 94%. In this paper, the model ensemble is applied to rock image identification. The features of the rock image are automatically extracted through the models AlexNet, VGG 16, Inception_V3, Xception, and ResNet50, and the classifier is constructed to classify the rock image automatically. The integrated model outputs the output results of a single model. Based on the voting method, it is integrated to determine the category of the rock image.

The oil content of rock is affected by a series of factors, such as petroliferous structure, rock type, material composition, diagenetic changes, and rock porosity and permeability, etc., which are the result of the combined effect of various factors (Liu et al, 2000). Traditional oil and gas detection technologies include geophysics and geochemistry, which are cumbersome and time-consuming. Petroleum has luminous characteristics under ultraviolet light. That is, the green or yellow part of the photos taken under fluorescent light contains oil. Based on this special rock sample image, this paper applies comprehensive image processing technology to calculate the oil-bearing area percentage of the rock to identify the oil-gas-bearing situation of the rock sample.

2. Rock Identification

2.1 Rock Sample Image

The sample data of the rock image is obtained by taking pictures of cuttings and core samples at the logging site using an industrial camera. Petroleum appears yellow or green when exposed to ultraviolet light. The rock image taken in white light in the dark box has features such as colour, texture, and granularity to identify lithology. There are seven types of rock sample images, as shown in figure 1.

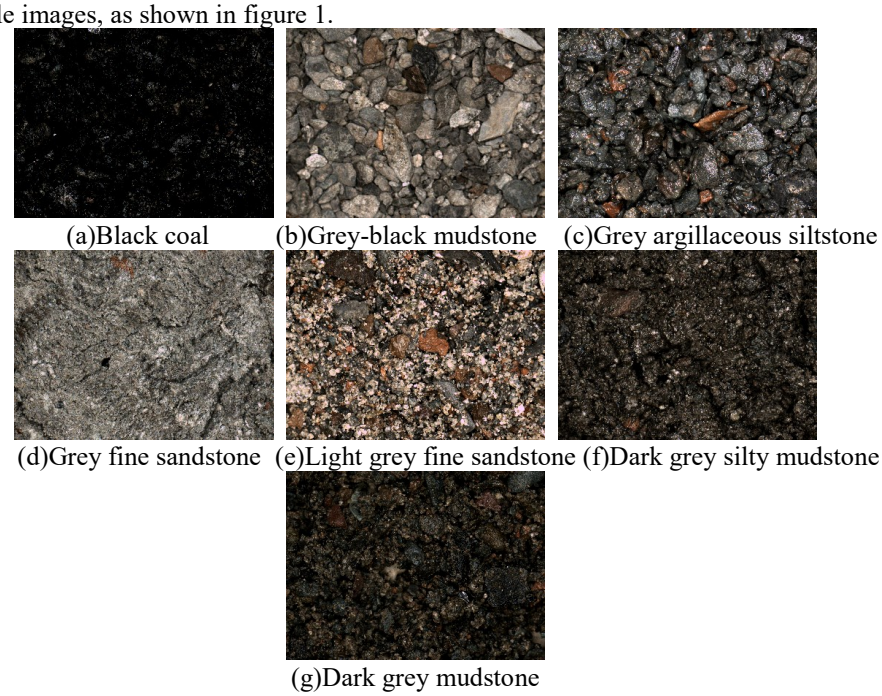

(a)Black coal (b)Grey-black mudstone (c)Grey argillaceous siltstone
(d)Grey fine sandstone (e)Light grey fine sandstone (f)Dark grey silty mudstone
(g)Dark grey mudstone

Fig. 1 Sample images of rocks in 7 categories

2.2 Building a Rock Identification Data Set

Before being used as the input of the training a convolutional neural network, the data is preprocessed first, as shown in figure 2. Some rock images in the original data set have irrelevant backgrounds. The irrelevant backgrounds are removed by cropping, and the invalid features are cropped to obtain data set 1; To increase the training sample set while ensuring the integrity of the texture as much as possible, a 30% overlapping cropping method is adopted to minimize the damage of the texture. Each image in data set 1 is cropped into four images, and data set 2 is obtained;

Considering that the computing power required for model training is limited to the hardware used in this experiment, to compress the amount of data while protecting the texture of the rock as much as possible, each image in the data set 1 is scaled to 0.1 times the original image. Each image of data set 2 is scaled to 0.2 times the original image. To take into account the global and local features of the rock image at the same time, the two are combined into a new data set 3; Since there are few rock sample images, operations such as random rotation, random adjustment of contrast, and random adjustment of brightness are used for data enhancement. For the balance of the sample set, different rock types are enhanced by different multiples, and data set 4 is obtained. Data set 4 is divided into training set and validation set according to the ratio of 8:2, as shown in Table 1.

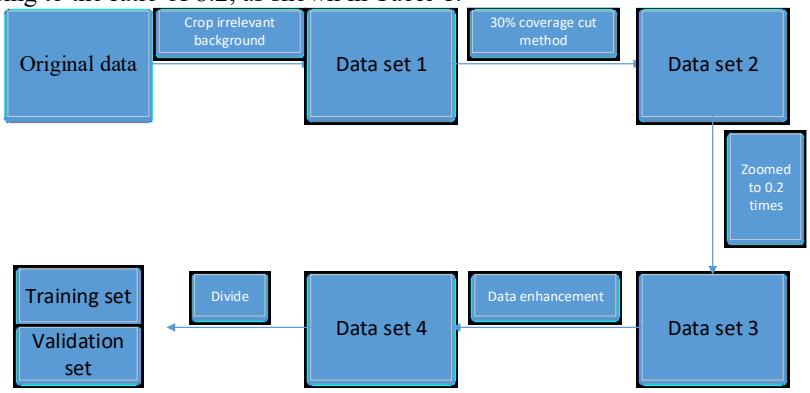

Fig. 2 Preprocessing of rock sample image data

Table 1 Type information and number of rock sample data sets

Serial number	category	Initial number	Number of training sets	Number of validation sets
a	Black coal	21	588	147
b	Grey-black mudstone	30	840	210
c	Grey argillaceous siltstone	46	920	230
d	Grey fine sandstone	18	576	144
e	Light grey fine sandstone	85	1020	255
f	Dark grey silty mudstone	40	800	200
g	Dark grey mudstone	75	900	225
sum	-	315	5644	1411

2.3 Convolutional Neural Network

The convolutional neural network can be divided into feature extraction and pattern recognition. Feature extraction is composed of convolution layer, activation function, and pool layer alternately. The first step is to use the output image from the previous layer of the convolution kernel. The convolution kernel is similar to the window used in image processing, which acts on the image and gets the feature map of the image by a convolution operation. A single image can use multiple convolution cores to perform convolution operations at the same time, which can extract more basic features of the image. Then the pooled layer performs a downsampling operation on the image to remove the redundant image information. Pattern recognition is a Multilayer perceptron classifier. After the image is processed by convolution and downsampling, features are obtained. These features are transformed into a one-dimensional vector, and the whole connection method is used as the input of the pattern recognition part to make the whole network recognize and classify. Figure 3 shows an example of a single convolution kernel for a single image.

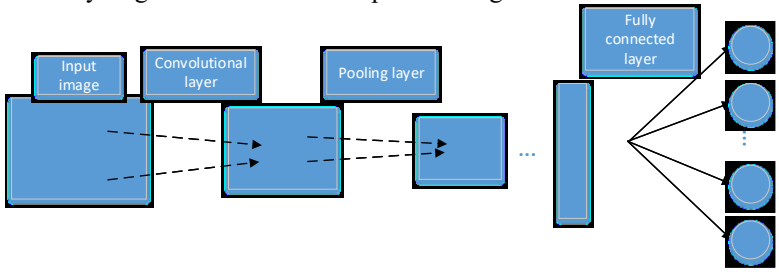

Fig. 3 Basic structure of CNN

2.3.1 AlexNet Model

The model, AlexNet, designed by Hinton and his students, won the international competition ImageNet in 2012. It can be said that AlexNet is both the successor and subvert of Lenet. First, it is using Relu as an activation function in an innovative way. Next, make a bold attempt to use the Dropout to solve the problem of over-fitting the model. Data enhancement was then used to fit the model with so many parameters. Finally, two gpus are used to speed up the convolution. In this paper, AlexNet model is trained, the activation function is used Relu, the complete connection layer is used Softmax classifier, the epoches are set to 150. The optimization function uses Adam with an initial learning rate of 0.0001. When the loss of the validation set did not decrease after ten iterations, the learning rate decreased to a minimum of 0.000001.

2.3.2 VGG16 Model.

Similarly, the model, VGG16, was featured in the ImageNet International Competition in 2014. Its input is 224X224X3 color image, the activation function learned from AlexNet, using the Relu function. Innovative use of a very small convolution kernel size makes the whole model simple. The training of VGG16 is consistent with the process of AlexNet.

2.3.3 Inception_V3 Model

The Inception_V3 network is an intense convolutional network developed by Google. Likewise, it was featured in the 2014 International Competition ImageNet, the first version of the inceptionnet. Google then developed a total of 4 versions of inceptionnet, of which Inception is the most representative. It not only learns from VGGNet, uses 3X3's convolution kernel, but also presents a regularization method-BatchNormalization for the first time. The training of Inception_V3 is consistent with the process of AlexNet.

2.3.4 Xception Model

Xception, also a model developed by Google, is an improvement on Inception_V3. In this paper, depthwise separable solution is introduced to improve the performance of the model without increasing the complexity of the network, and the number of parameters is similar to Inception_V3. Therefore, the goal of Xception is not model compression, but improved performance. The training of Xception is consistent with the process of AlexNet, but the epoches have been reduced to 100. The change of the loss of the training set and the validation set during the iteration process is shown in figure 4.

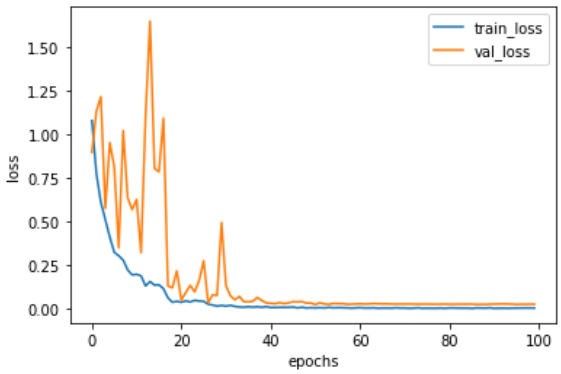

Fig. 4 Loss changes

2.3.5 ResNet Model

The model ResNet won first place in the ImageNet International Competition in 2015 for its superior classification accuracy. It is a residual network, both simple and practical. When solving the traditional machine learning problem, all the samples are taken as input, and the model parameters are trained from scratch, which takes a lot of time and computational cost. When two tasks have some correlation, we can use the model parameters obtained from the training of the previous task to the current task, which is called migration learning. This approach is often efficient for small data samples. Migration learning includes pre-training networks and fine-tuning.

Pre-trained network: model parameters saved by training the sample set (large-scale image classification tasks, such as ImageNet). If the sample set is large and contains everything, the model parameters trained by the pre-training network can be directly used as the parameters of the current task using the model. Even if the new problem and the new task are completely different from the original task, the learning characteristics are transplantable between the different problems, which is the characteristic of transfer learning. The pre-training networks built into Keras include

VGG16, VGG19, ResNet50, Inception_V3, Xception, and so on.
Fine-tuning: first, freeze all network model parameters, then, according to the current task requirements, unfreeze several layers of network, add classifier. Only when the classifier has been trained can the top convolutional layer of the convolutional base be fine-tuned. If this is not the case, the initial training error is huge, and the representations learned by these convolutional layers before fine-tuning will be destroyed. Finally, the model is built by training the current sample set, which greatly reduces the time and computational cost.
In this paper, ResNet50 is used as the pre-training model and fine-tuned. The model is shown in figure 5. Use data4 for training and validation set for testing. The evaluation indicators use accuracy, macro-P, recall macro-R, and macro-F1. After thawing the three layers, the last nine layers, the last 19 layers, and all thawing, the results are shown in Table 2.

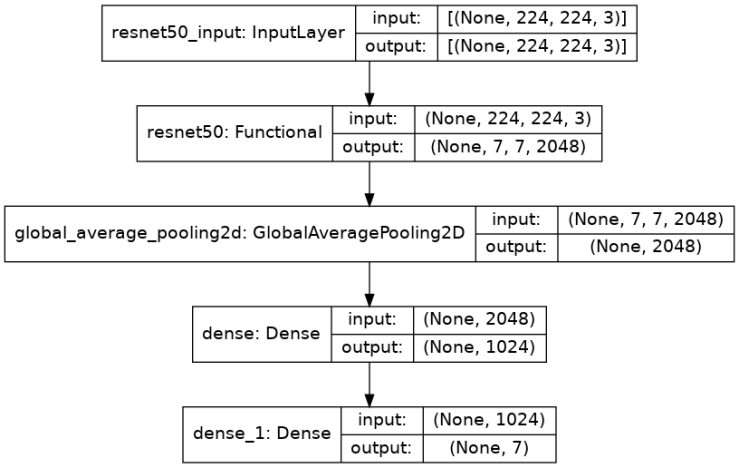

Fig. 5 ResNet50 migration learning model

Table 2 ResNet migration learning effect

Thawing layer	accuracy	macro-P	macro-R	macro-F1
3	0.4954	0.5188	0.5180	0.5184
9	0.5145	0.5395	0.5459	0.5427
19	0.5145	0.5560	0.5499	0.5529
all	0.9440	0.9532	0.9477	0.9504

Since the similarity of the rock image data set in this article is far from that of the ImageNet data set, it is better to train the ResNet model with the rock image data set in this article after all thawing.

2.3.6 Model Integration

The result of synthesizing multiple learners is integrated learning. At the heart of this is how to train multiple powerful but different learners. On specific issues, ensemble learning is usually better than a single model, and is popular with scholars in some international competitions.
The model integration is the fusion of multiple trained models, based on a certain way to achieve multi-modal fusion of test data so that the final result can "learn from each other's strengths", integrate the learning capabilities of each model, and improve generalization ability of the final model. In recent years, the model ensemble has become an artefact in kaggle, tianchi and other competitions. It can be used in image segmentation, classification, detection and other fields. The model integration method is mainly applied to the large differences and small correlations of several models. This effect is more obvious. Commonly used model ensemble methods are voting, averaging, stacking, and blending.
Among all integrated learning methods, the most intuitive is majority voting. Because its purpose is to output the most popular (or most popular) prediction among the basic learner's predictions. Voting is the simplest and most intuitive integration method. It's the result of counting multiple learners, and the one with the most is the end result. Similar to voting in an election, the learner is the voter, and the category is the competitor. There are two main ways to combine multiple predictions with voting: hard voting, and the other is soft voting.
This article adopts the complex voting method (figure 6), our common principle of "the minority obeys the majority". We can count the classification results of multiple models, which category has a high frequency, that is, which category is selected. On the basis of the same sample set, several different but powerful classifiers are established. The final decision is then made by voting with a majority in favor of a minority. Suppose there are five models, and the classification of a particular data is 1, 1, 1, 2, and 2. The voting result is 1. The models AlexNet, VGG16, Inception_V3, Xception, and ResNet50 are selected as the base classifiers for model integration, and their results are

integrated based on the voting method.

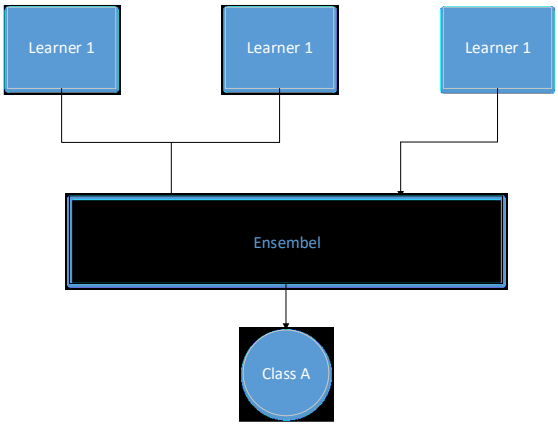

Fig. 6 Hard voting

3. Identification of Oil and Gas

Petroleum appears yellow or green when exposed to ultraviolet light. Fluorescent rock images are taken in the dark box to extract the oil-bearing area to identify the oil-gas-bearing situation of the rock. The rock image contains irrelevant background, so when calculating the oil content of the rock, first extract the part of the area occupied by the rock from the image and then perform the next step.

Fig. 7 Fluorescent rock image

3.1 Thresholding

To get the binary image, under the rule of pixel distribution of the image, the threshold is set to segment the pixel, which is called the threshold segmentation of the image. In OpenCV, an image processing library, there are threshold functions: threshold, which are used for threshold segmentation. Figure 8 shows the thresholded images obtained by selecting different method parameters. The visible parameter TOZERO_INV is suitable for rock images.

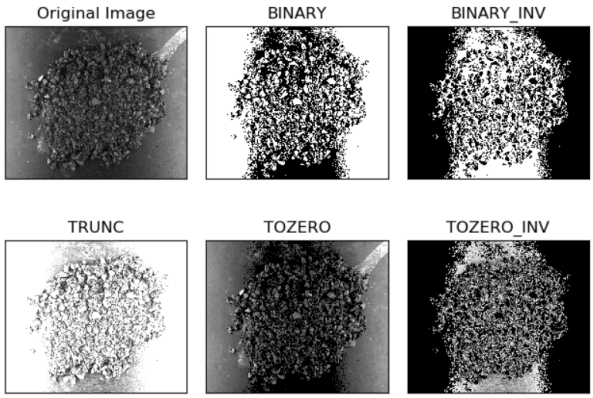

Fig. 8 Image thresholding

3.2 Edge Detection

When you need the basic contour of an image, you can use edge detection. Image Edge detection can reduce the amount of data, but also can remove irrelevant information, and finally preserve the important structure of the image attributes. It can be said that edge detection is a filter, different operators and any combination of different images will get different results. There are basically three operators, Sobel operator, Laplacian operator, and Canny operator.

Canny operator is not sensitive to noise and performs well in edge detection. Its characteristic is that it can detect both the real edge and the weak edge with different thresholds. In this paper, Canny operator is used for image edge detection.

3.3 Image Expansion

The image expansion process adds pixel values to the edges of the image to expand the overall pixel value and then achieve the image expansion effect, which can also be said to be pixel interpolation processing. In a mathematical sense, the image expansion operation is a convolution operation on the image (X) with the kernel (B). The anchor point can be any shape and size, but only one, the individually defined reference point. The nucleus is generally a solid disk with a reference point in the center. Using the kernel as a template, the kernel and the image is convoluted to calculate the maximum pixel value of the kernel region and assign it to the pixel specified by the reference point. Finally, the highlights of the image can be inflated. As shown in figure 9, this is the convolution operation for image inflation.

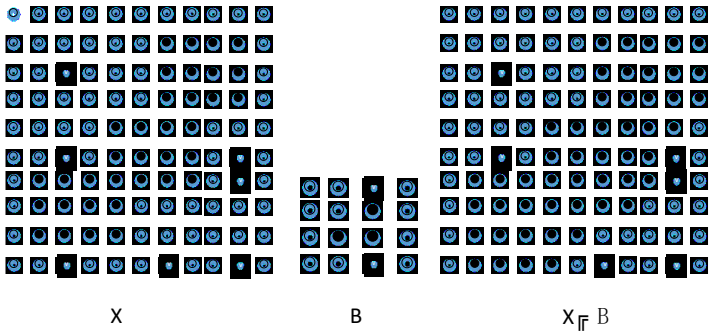

Fig. 9 Expanded convolution operation

3.4 ENVI Extraction Verification

In machine vision and image processing, the area to be processed is outlined in boxes, circles, ellipses, irregular polygons, etc., from the processed images, which are called regions of interest. To divide the area of interest, the remote sensing image processing software ENVI (The Environment for Visualizing Images) can be used. It can be applied to many aspects of image data input/output, calibration, image enhancement and so on.

3.5 HSV Conversion

Since the oil is green and yellow under fluorescence, it is necessary to calculate the percentage of the area occupied by green and yellow in the total area. Then first, determine the range corresponding to green and yellow. There are two commonly used methods to determine colours, RGB and HSV. Here I use HSV. HSV is a colour space created based on the intuitive characteristics of colours, also called the Hexcone Model. The colour parameters in this model are hue (H), saturation (S), and lightness (V).

Table 3 HSV colour classification

	black	grey	white	red		orange	yellow	green	cyan-blue	blue	Purple
h-min	0	0	0	0	156	11	26	35	78	100	125
h-max	180	180	180	10	180	25	34;	77	99	124	155
s-min	0	0	0	43		43	43	43	43	43	43
s-max	255	43	30	255		255	255	255	255	255	255
v-min	0	46	221	46		46	46	46	46	46	46
v-max	46	220	255	255		255	255	255	255	255	255

The HSV colour classification is shown in Table 3. The yellow corresponds to the range (26, 43, 46) to (34, 43, 255), and the green corresponds to the range (35, 43, 46) to (77, 43, 255). The combination of those is the threshold (26, 43, 46) to (77, 43, 255) used this time. The image where the HSV value is within the threshold is the required rock oil content part.

4 Experiment and Result Analysis

4.1 Analysis of Image Recognition Problems

4.1.1 Model Training

This article uses models AlexNet, VGG16, Xception, Inception_V3, ResNet50 for training. It uses the function ImageDataGenerator in Keras to enhance the data during the training process, expand the size of the data set, and enhance the generalization ability of the model. Table 4 shows the performance effects of the five models on the validation set. Table 5 shows the accuracy of the five models on different rock types in the verification set.

Table 4 Evaluation indicators of 5 models

Model	Accuracy	Macro-P	Macro-R	Macro-F1
AlexNet	0.9532	0.9538	0.9571	0.9555
VGG16	0.9596	0.9637	0.9622	0.9629
Xception	0.9880	0.9883	0.9890	0.9886
Inception_V3	0.9887	0.9888	0.9896	0.9892
ResNet50	0.944	0.9532	0.9477	0.9504

Table 5 The accuracy of different rock types on the validation set

Model	a	b	c	d	e	f	g
AlexNet	1	0.9714	0.9696	0.9931	0.9529	0.915	0.8978
VGG16	1	0.9667	0.9826	0.9722	0.9686	0.97	0.8756
Xception	1	1	0.9957	1	0.9961	0.98	0.9511
Inception_V3	1	0.9952	1	1	0.9961	0.985	0.9511
ResNet50	1	0.9667	0.987	0.9792	0.9686	0.91	0.8222

It can be seen from Table 4 that the recognition accuracy of the model Inception_V3 is higher, reaching 98.87%, and the effects of the other models are also sound. As shown in Table 5, the model's recognition of type a rocks reached 100%, and the recognition rate of type g rocks was generally low, and type g rocks were mistaken for type c and type e.

4.1.2 Model Integration

Integrate models with better performance in image rock recognition. The evaluation indicators are shown in Table 6. The recognition results of models VGG16, AlexNet and ResNet50, are integrated based on voting, which can achieve a recognition accuracy of 97.51%; model Xception and VGG16 Integration with AlexNet can achieve a recognition accuracy of 98.72%; integrating the models Xception, VGG16, and Inception_V3, the recognition accuracy can reach 99.29%, model integration has higher recognition capabilities, and integrated models have higher performance and better stability.

Table 6 Model integration recognition effect on the validation set

Model1	Model2	Model3	Accuracy	Macro-P	Macro-R	Macro-F1
VGG16	AlexNet	ResNet50	0.9751	0.977	0.9762	0.9766
Xception	VGG16	AlexNet	0.9872	0.9877	0.9881	0.9879
Xception	VGG16	Inception_V3	0.9929	0.9932	0.9935	0.9933

Integrate 5 models (Inception_V3, VGG16, AlexNet, ResNet50, Xception), the evaluation indicators are: 0.9894 (Accuracy), 0.9902 (Macro-P), 0.9903 (Macro-R), 0.9902 (Macro-F1). The effect of the integration of the five models is not enough for the effect of the integration of the three models, indicating that the integration is not that the more models, the better. Still, the recognition effect of the model itself must be investigated.

4.2 Analysis of Rock Oil Content

4.2.1 Rock Area Extraction

This paper uses an edge detection algorithm to extract the part of the rock in the image. The specific operation is as follows: To enhance the image characteristics, first, use 2% linear stretching for figure 7, and then convert the linear stretching result image into a grayscale image, and use the cv2.threshold method according to the preset threshold to change the processed pictures are converted into binarized pictures for edge detection. Subsequently, the Canny edge detection algorithm performs edge detection on the obtained binary image, and figure 10 is obtained. It can be seen that the edge detection result at this time does not meet the requirements. To further optimize the result, use the idea of image expansion, use the cv2.dilate method to expand the image, and then use cv2.drawContours to fill the outline colour, set the background to black, set the interior to white, and to remove the noise when filling, it must be processed

For small contour areas, then repeat contour extraction, image expansion, contour filling and other operations, and finally get figure 11.

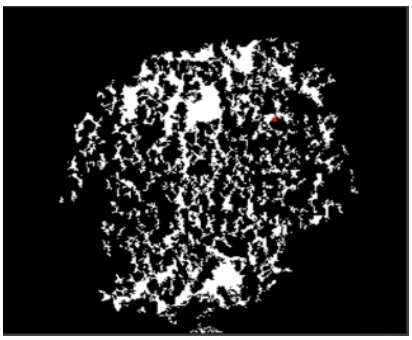

Fig. 10 Edge detection

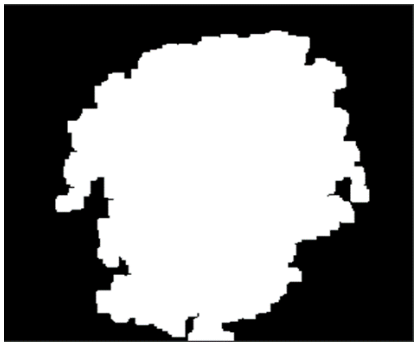

Fig. 11 The final result

To judge whether the extracted contour is accurate, it can be judged from two aspects: intuitive estimation and data comparison. To intuitively compare the obtained contour with the original image, the extracted contour can be superimposed on the original image. The result is shown in figure 12, which shows that the contour can better cover the stone part.

At the same time, the accuracy of the method used in this paper to extract the rock area is verified, and the rock art in the image is selected as the area of interest using the ENVI software. The result is shown in figure 13. In this paper, the method of calculating pixels is used to calculate the area. At this point, it can be calculated that the image (figure 7) contains a total of 5013504 pixels, the number of pixels in the extracted contour (the white part of figure 15) is 2379526. The region of interest (the red part of figure 13). There are 2400770 pixels in total, and the number of pixels corresponding to the extracted contour is similar. Therefore, it can be concluded that directly using the total pixels of the map to calculate the percentage of the oil-bearing area will bring more significant errors. The number of pixels occupied by the contour obtained by the rock mentioned above area extraction method can obtain a more accurate result.

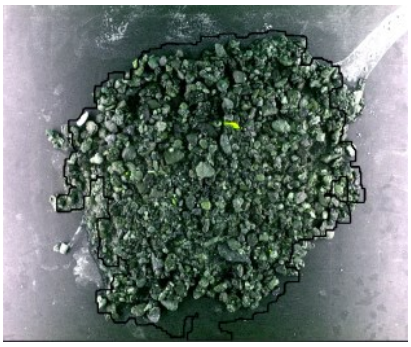

Fig. 12 Comparison of the extracted contour and the original image

Fig. 13 ENVI extracts the area of interest

4.2.2 Rock oil content extraction

After the extraction of the rock profile on image 7 is completed, the oil-bearing area percentage of the rock is calculated. The same idea is to use the mask. The specific operation is as follows: first, convert the picture into HSV colour space, and then use the previously set threshold to binarize the picture into a black or white form, where the black area means to delete the pixels in this area, and white means to keep the pixels in this area. The value for black is 0, and the value for white is 255. And this is the mask corresponding to the picture, and Fig. 14 is the mask corresponding to Fig. 7.

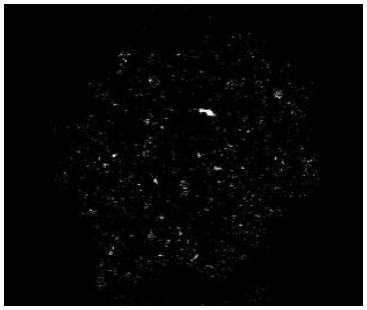

Fig. 14 The mask of the rock image

After successfully obtaining the mask, you can start processing. Use np.count_nonzero to obtain the pixels in the mask area, which is occupied by the yellow-green part. Then divide the area occupied by the yellow-green part by the total area to get the oil-bearing area percentage of the rock. The total number of pixels in the image is 2587694, the number of pixels in the oily part is 73758, and the final percentage is 2.85%.

5 Summary and Outlook

This article first analyzes the cumbersome and complicated traditional classification of rocks at this stage, introduces the current most classic convolutional neural network, and uses it in the training data set to perform model integration to improve the effect of rock image classification. First, extract the rock area from the image, and then extract the oil-bearing area from the image to calculate the oil content of the rock image. The reason why the accuracy of rock image recognition on the verification set is so high is that the data augmentation makes the training set and the verification set too correlated, the image repeatability is high, and the preprocessing of the data needs to be further improved.

Acknowledgment

This work was funded by National Natural Science Foundation of China under contract No. 41771384 , National Key Research and Development Projects under contract No. 2016YFC1401203, Provincial Special Funds for Economic Development (use of marine economic development) in 2018 under contract No.GDME-2018E003.

References

Zou Qi, He Yueshun, Yang Xi, 2020. Construction of lithology identification model by well logging based on ensemble learning [J]. Intelligent Computers and Applications, 10(03), pp. 91-94.
Cheng Guojian, Guo Wenhui, Fan Pengzhao, 2017. Study on rock image classification based on convolutional neural network[J]. Journal of Xi'an Shiyou University (Natural Science Edition), 32(04), pp. 116-122.
Ren Wei, Zhang Sheng, Qiao Jihua, 2021. The rock and mineral intelligence identification method based on deep learning[J]. Geological Review, 67(S1), pp. 281-282.
Bai Lin, Wei Xin, Liu Yu, 2019. Rock thin section image recognition and classification based on VGG model[J]. Geological Bulletin, 38(12), pp. 2053-2058.
Zhang Ye, Li Mingchao, Han Shuai, 2018. Automatic identification and classification in lithology method based on deep learning in rock images[J]. Acta Petrologica Sinica, 34(02), pp. 333-342.
Hu Qicheng, Ye Weimin, Wang Qiong, 2020. Recognition of lithology with big data of geological images[J]. Journal of Engineering Geology, 28(06), pp. 1433-1440.
Cheng Guojian, Fan Pengzhao, 2018. Analysis of rock granularity by deep belief network[J]. Journal of Xi'an Shiyou University (Natural Science Edition), 33(03), pp. 107-112.
Polat, Özlem, Polat, 2021. Automatic classification of volcanic rocks from thin section images using transfer learning networks[J]. Neural Computing and Applications, 33(18).
Feng Yaxing, Gong Xi, Xu Yongyang, 2019. Lithology recognition based on fresh rock images and twins convolution neural network[J]. Geography and Geo-Information Science, 35(05), pp. 89-94.
Li Yang, Huang Wei, Xi Jianzhong, 2021. NOx emission forecasting based on stacking ensemble model[J]. Thermal Energy and Power Engineering, (05), pp. 73-81.
Feng Hailin, Hu Mingyue, Yang Yinhui, 2019. Tree species recognition based on overall tree image and ensemble of transfer learning[J]. Transactions of the Chinese Society of Agricultural Machinery, 50(08), pp. 235-242.
Zhang Chen, Du Gang, Du Xuetao, 2017. Illegal image classification based on ensemble deep model[J]. Journal of Beijing Jiaotong University, 41(06), pp. 21-26.
Liu Yongjian, Shen Jun, Liu Yijian, 2000. An artificial neural network based method for evaluating the oil prospects of rocks[J]. Petroleum Geology & Experiment, (03), pp. 276-279.